

Texas Southern University

## Digital Scholarship @ Texas Southern University

---

Faculty Publications

---

1-1-2020

### Thermal degradation of azobenzene dyes

Thao L. Nguyen

*Texas Southern University*

Mahmoud A. Saleh

*Texas Southern University*

Follow this and additional works at: <https://digitalscholarship.tsu.edu/facpubs>

---

#### Recommended Citation

Nguyen, Thao L. and Saleh, Mahmoud A., "Thermal degradation of azobenzene dyes" (2020). *Faculty Publications*. 81.

<https://digitalscholarship.tsu.edu/facpubs/81>

This Article is brought to you for free and open access by Digital Scholarship @ Texas Southern University. It has been accepted for inclusion in Faculty Publications by an authorized administrator of Digital Scholarship @ Texas Southern University. For more information, please contact [haiying.li@tsu.edu](mailto:haiying.li@tsu.edu).



## Thermal degradation of azobenzene dyes

Thao L. Nguyen, Mahmoud A. Saleh\*

Department of Chemistry, Texas Southern University, Houston, TX, USA

### ARTICLE INFO

#### Keywords:

Thermochemistry  
Free radicals  
Aromatic amines  
TGA  
Azo dyes  
GCMS

### ABSTRACT

Ten azobenzene dyes were tested for their thermal degradation products from ambient temperature to 800 °C using a thermogravimetric technique. Degradation products were analyzed at each 100 °C increment using gas chromatography-mass spectrometry. Products were identified based on their mass spectral data and their retention times. Thermal degradation from all dyes resulted in loss of the azo group as nitrogen gas and aromatic free radicals. Electron withdrawing groups enhance the dissociation of the phenyl nitrogen bond at the benzene moiety carrying the electron withdrawing group. On the other hand, electron donating groups inhibited the dissociation of the phenyl-N bond of the benzene moiety carrying the electron donating groups. The loss of nitrogen molecule from the dyes appeared to be taken place in a two-step rather than a one-step reaction in which the phenyl nitrogen bond of the phenyl group carrying the electron withdrawing group splits to form phenyl and azo phenyl radicals following by the loss of a nitrogen molecule and a new phenyl radical. This was also supported by calculating degradation reaction enthalpies and bond dissociation energies using density functional theory quantum mechanics.

### 1. Introduction

Azo dyes are synthetic organic colorants, characterized by the chromophore azo groups ( $-N=N-$ ). They have been extensively used in numerous industrial applications due to their colorfastness and low price. Currently, there are over 3000 azo dyes in use worldwide and they account for 70% of the commercial dye market [1,2]. These dyes offer a wide spectrum of colors and are used for coloring a variety of consumer goods, such as food, pharmaceutical, textile, leather, clothes, toys, plastics, and cosmetics [3–5]. Additionally, they are used as photo functional materials for optical devices, photovoltaic cells, and biosensors [6,7]. Most of these dyes are easily synthesized from inexpensive and easily obtained starting materials and encompass the entire visible spectrum, amenable to structural modification, and can be made to bind to most synthetic and natural materials. The global production of textile dyes was believed to exceed 1 million tons in 2020 [2]. Within the azo dye group, azobenzene dyes are one of the most fundamental and useful organic dyes owing to their color tunability based on facile modulation of the molecules [8].

It is estimated that more than 15% of the azo dyes are released into the environment as wastewater during textile processing or as solid waste from home or industrial uses [9–11]. Dyes are designed to be resistant to light, water and oxidizing agents, so it is difficult to remove them once they are released into the environment. Azo dyes are

susceptible to release carcinogenic amines under environmental conditions [12–14]. Several epidemiological studies have demonstrated that the exposure to azo-based dyes has caused cancer in humans [15–18]. Colored wastewater resulting from the loss of up to 40% of the dye during the dyeing process is passed to wastewater treatment plants or into the environment [19–21]. Therefore, the health issues of azo dyes have received much attention in recent years. Photochemical degradation and metabolisms of azo dyes by microorganisms and animals including humans and subsequent release of aromatic amines are well documented [22–27], however, much less information is available for thermal degradation of azo dyes and the formation of aromatic amines. Knowledge about thermal degradation of azo dyes and the release of suspected carcinogenic aromatic amines is crucial for dealing with accidental fire in warehouses or storage facilities containing materials having azo dyes components such as fabrics, plastics or raw materials. It may also be relevant that some of the azo dyes that are used for food coloring may release aromatics amines during cooking.

In this study we selected 10 azobenzene dyes containing different types of electron donating (donor) and electron withdrawing (acceptor) groups to study their thermal degradation at temperatures ranging from room temperature to 800 °C using the thermogravimetric analysis technique (TGA). Thermal degradation products were identified at different temperature segments using the inline gas chromatography-mass spectrometry technique (GCMS).

\* Corresponding author.

E-mail address: [mahmoud.saleh@tsu.edu](mailto:mahmoud.saleh@tsu.edu) (M.A. Saleh).

## 2. Materials and methods

### 2.1. Chemicals and supplies

All chemical reagents, solvents and the ten azobenzene analytical standard dyes with purity greater than 96% were purchased from Millipore Sigma (St. Louis, Mo 63178 USA).

### 2.2. Thermogravimetric analysis (TGA)

Thermogravimetric analyses (TGA) were recorded using a NETZSCH TGA (209 F1) thermal analyzer (Netzsch–Germany) under nitrogen gas. The tests were performed in  $\text{Al}_2\text{O}_3$  pans with  $5.0 \pm 0.5$  mg samples and heated from 25 °C up to 800 °C at a heating rate of 50 °C/min. The gases released during thermal decomposition were transferred to GCMS instrument using quartz capillary line (75 mm diameter and 2 m long) at 290 °C. The instrument assembly is shown in Fig. 1.

### 2.3. Gas chromatography-mass spectrometry (GCMS) analysis

TGA products were analyzed using Agilent 7890B/5977A GCMSD system (Agilent Technologies) equipped with an HP-5 MS 5% diphenyl–95% dimethylpolysiloxane capillary column 30 m  $\times$  0.25 mm, 0.25  $\mu\text{m}$ . Helium was used as the carrier gas with gas flow rate of 1.0 mL/min. The temperatures of the injector, transfer line, and ion source were 230 °C, 250 °C, and 230 °C, respectively in splitless mode, GC oven temperature was kept constant (isotherm) at 150 °C. Mass spectral acquisitions were performed in electron ionization (EI) mode at 70 eV. The post-run analyses were performed by Masshunter software Qualitative Analysis B.07.00 SP1. Chemicals were identified based on their retention times and mass spectra search using NIST 17 database.

### 2.4. Computational assessment

All quantum chemical calculations were carried out using the density functional theory (DFT) wB97X-V or B97M-V with 6–311 + G(2 df,2p) [6-311G\*] method in the Spartan 18 program package (Wavefunction, Inc. Irvine, CA, U.S.A.).

## 3. Results and discussion

Chemical structures of the tested azobenzene dyes are shown in Fig. 2. Four of the tested dyes exhibited tautomerism structure, sudan orange G (Dye #1) and chrysoidine G (Dye #2) having three possible tautomers with possible intramolecular hydrogen bonding stabilization, disperse yellow 3 (Dye #7) have 3 tautomers but no hydrogen bonding, and aniline yellow (Dye # 4) have 2 tautomer with no possible intramolecular hydrogen bonding.

### 3.1. Thermogravimetric analysis (TGA)

The data from the NETZSCH TG 209 analyzer are divided into four groups: temperature (°C), time (s), weight loss (%) (described as  $w/w_0$ ) as shown in Fig. 3, and first derivative of weight loss with respect to time shown in Fig. 4. In order to compare the different susceptibility of the tested azo dyes for thermal degradation, the data of the TG and DTG were calculated according to the equation:

$$TG = \alpha = \frac{w - w_0}{w - w_\infty} \text{ and } DTG = \frac{dw}{dt}$$

Where  $w$  is the weight of sample in the TGA experiment at time  $t$ .  $w_0$  is the initial weight of the sample,  $w_\infty$  is the final weight of the sample.  $\alpha$  is described as the rate of thermal degradation. Dyes # 3 and 4 showed similar behavior and degraded quickly to complete weight loss at temperature less than 265 °C (Fig. 2) which was also seen in Fig. 4 as the fastest rate of degradation. The two dyes having similar chemical structures but dye 4 has further stabilization by tautomerism which shown slightly higher stability than dye 3 that lack

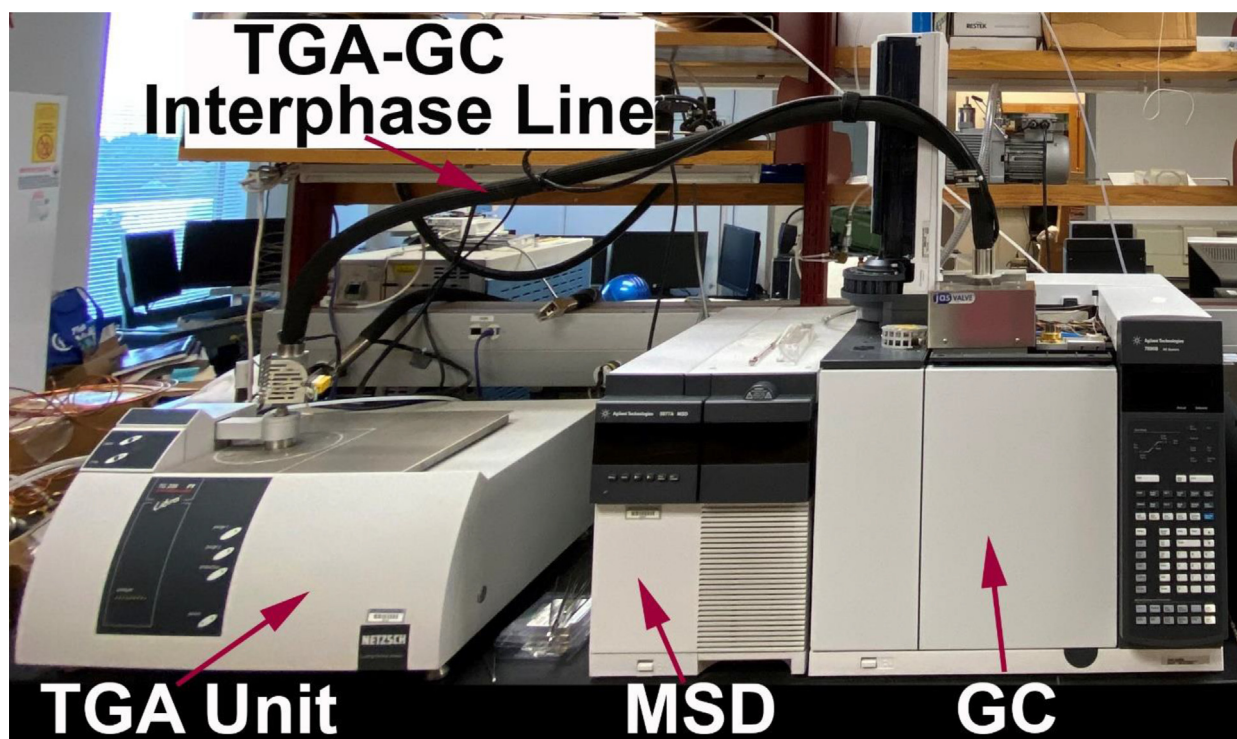


Fig. 1. TGA/GCMS assembly.

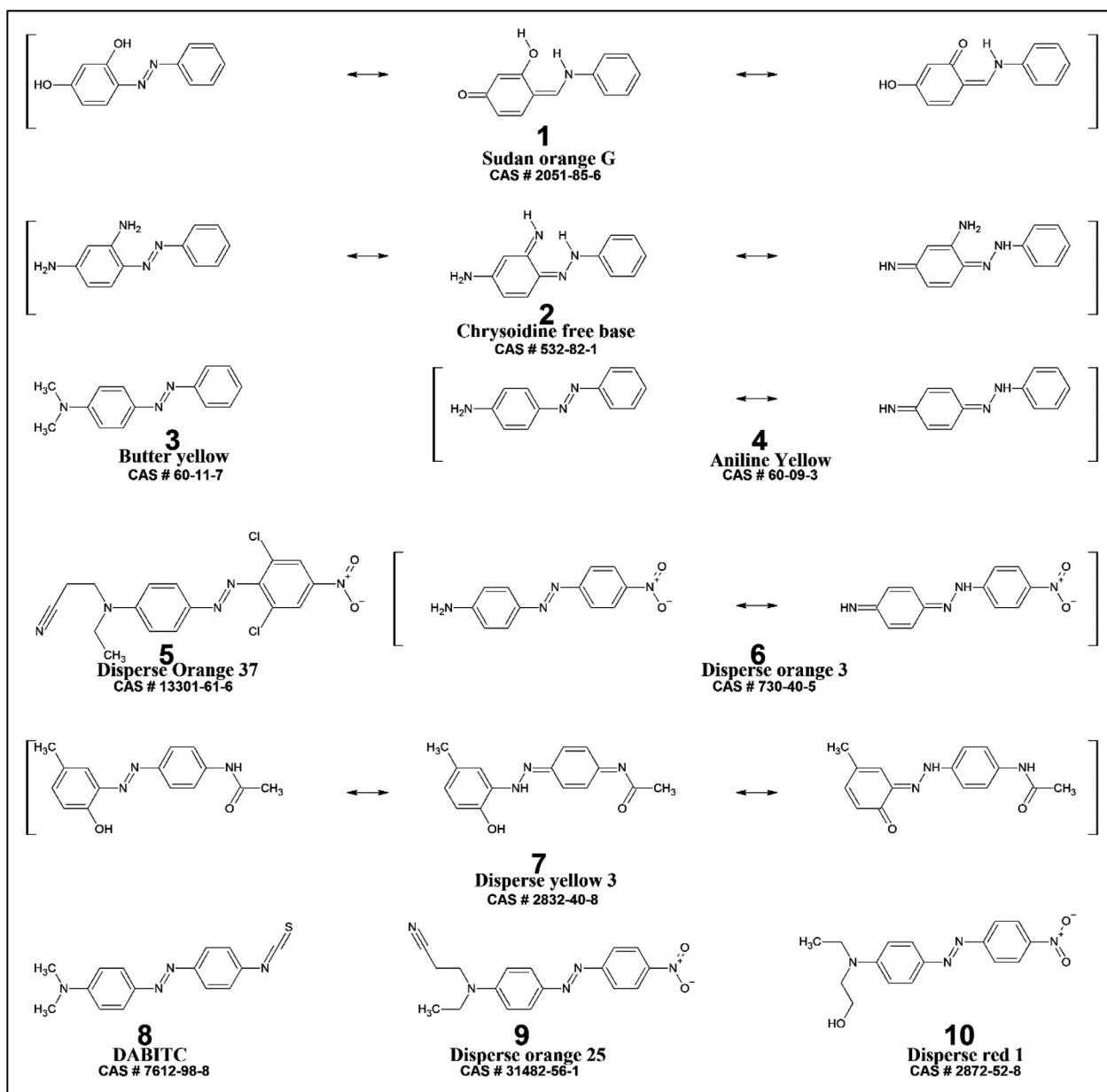


Fig. 2. Chemical structures of the tested azobenzene dyes.

tautomerism. Dyes #8 and 9 also were similar and were totally lost at 300 °C and 320 °C, respectively, and followed by dye #10 but at much lower rate than dyes 3, 4, 8, and 9. The next cluster included two dyes # 6 and 1 where they fully degraded at a temperature of 500 °C and 600 °C, respectively, dye #1 was more stable than dye # 6 which is consistent with the fact that dye #1 has three tautomers with stronger intramolecular hydrogen bonds, however, dye # 6 showed two possible tautomers but no hydrogen bonds. Dyes #2, 5, and 7 showed the lowest rate of thermal degradation and only dye #2 showed a 100% weight loss at 790 °C, however, dyes # 5 and 7 never reached 100% weight loss even at 800 °C. Table 1 showed a summary of all of thermal decomposition pattern including the experimental melting point of each dye. TGA and DTG results are shown in Figs. 3 and 4.

### 3.2. Gas chromatography mass spectrometry (GCMS) analysis

Thermal degradation chemical products obtained from the TGA experiment were continuously analyzed by GCMS. Products were

collected as a cluster at each 100 °C increments (every 2 min), each cluster were identified using NIST library search and retention time matching with external standards. Fig. 5 is an illustrated example for TGA/GCMS analysis of the dye sudan orange G (dye #1). It appears from the total ions chromatogram (TIC) that more than 60% of the products were produced between 200 °C and 300 °C consistent with the DTG data shown in Fig. 4 and Table 1.

Chemical identified thermal decomposition products and their relative concentration at each 100 °C segments for all the tested dyes are shown in Table 2. Chemicals below molecular mass of 50 such as H<sub>2</sub>O, N<sub>2</sub> and CO<sub>2</sub> were not analyzed.

Dyes # 1, 2, 3, and 4 the contain electron donating groups (donor) at only one benzene ring with the second benzene group carrying no substituent, all of them were found to be the fastest in degrading at temperature lower than all of the other dyes at temperature less than 240 °C (as seen in Fig. 4 and Table 2). Indicating that dyes 1 to 4 are the most susceptible to degradation and all of them showed the formation of benzene in the early stages of degradation indicating that the

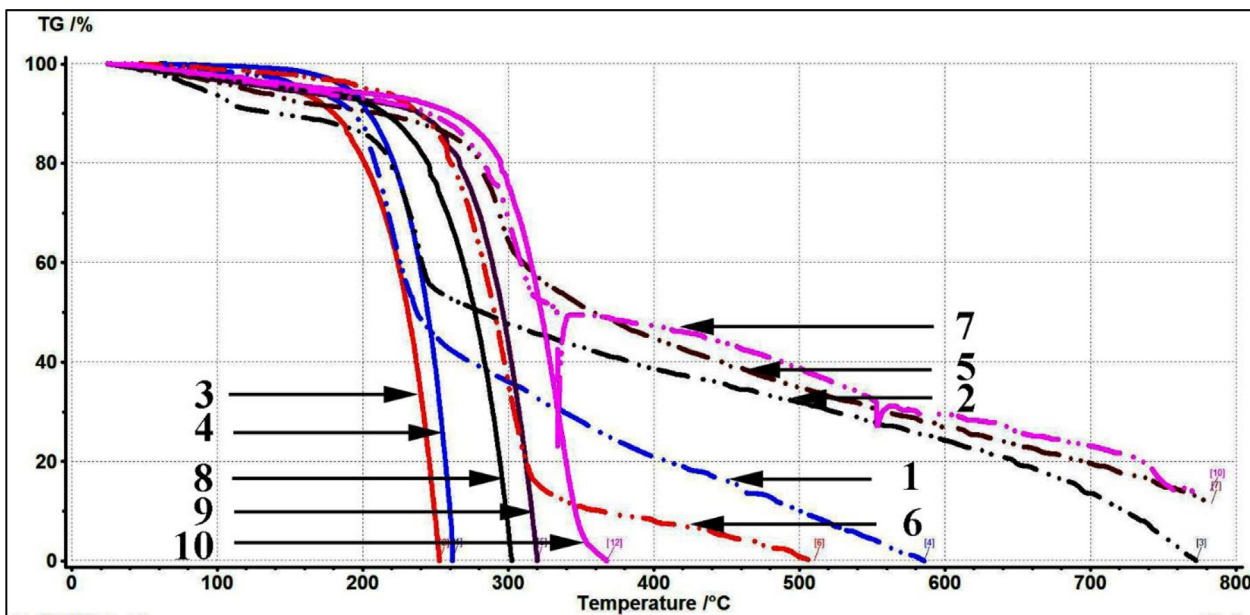


Fig. 3. Thermogravimetric analysis of the tested 10 azobenzene dyes, showing weight lost as a function of temperature, numbers on each trace represent the specific dye shown in Fig. 2.

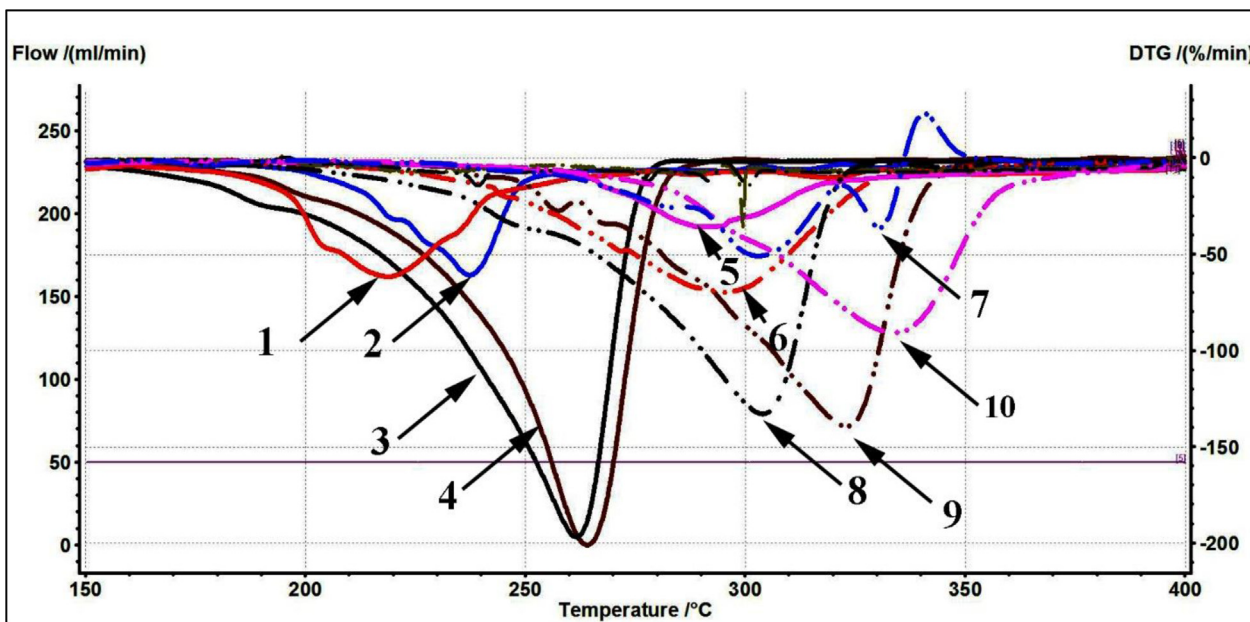


Fig. 4. Rate of weight loss as DTG%/min as a function of temperature.

Table 1  
Thermal characterization of azobenzene dyes.

Dye #	TG Temperature Range (°C)	DTG Peak (°C)	DTGA (%/min)	MP (°C)
1	50–600	218.9	61.5	170
2	50–785	237.2	60.5	118
3	50–250	261.3	196.9	117
4	50–260	263.4	200.54	127
5	150–800	289.5	35.32	145
6	120–800	294.7	69.85	215
7	200–500	331.2	22.5	195
8	250–800	303.8	133.02	170
9	100–305	330.2	132.8	170
10	150–370	333.6	96.77	161

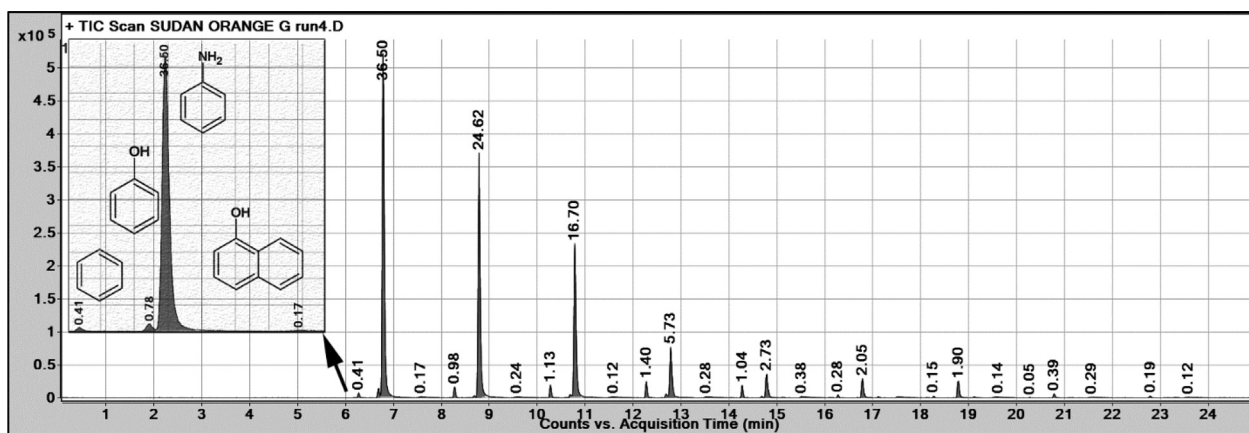


Fig. 5. Total ion chromatogram of thermal degradation products from Sudan orange G dyes, collected every 2 min, with a zoom at the first cluster for peak identification. Numbers above each peak represent the normalized percentage peak area.

Table 2

TGA products identified at different temperatures using GCMS. Values shown for each dye represent the normalized area % for each peak in the total ions chromatogram (TIC).

Products	TGA Temperature, °C							
	100	200	300	400	500	600	700	800
<b>Sudan orange G (2,4-Dihydroxyazobenzene), Dye # 1</b>								
Benzene		0.4	0.98	1.1	1.4	1.0	0.3	0.2
Phenol		0.8	0.2	0.2	0.4	0.1		
Aniline		36.5	24.6	16.7	5.7	2.7	2.1	1.9
a-Naphthol				0.3	0.2	0.1		
<b>Chrysoidine G (4-Phenylazo-m-phenylenediamine), Dye # 2</b>								
Benzene		12.3	1.2	1.0	1.0	0.6		
Aniline		11.0	28.2	7.14	5.14	1.5	0.6	
Diaminobenzene		6.9	1.0					
<b>Butter yellow (4-Dimethylaminoazobenzene), Dye # 3</b>								
Benzene		4.1						
Aniline		4.5	7.1	5.0	3.2	0.9		
N, N-dimethylaniline		21.5	4.9	3.9	4.0	3.1	4.9	
<b>Aniline yellow (4-Aminoazobenzene), Dye # 4</b>								
Benzene		2.2						
Aniline			8.7	12.7	6.6	2.1	1.5	
Diaminobenzene			8.6	8.3	1.2			
<b>Disperse Orange 37 (3-[4-[2,6-dichloro-4-nitrophenyl]iazinyl-N-ethylaniline]propanenitrile), Dye # 5</b>								
CH <sub>2</sub> = CHCN		20.4	18.9	8.8	3.4	2.3	1.1	0.8
3,5-dichloronitrobenzene					0.1	0.3	0.3	0.2
3-(ethylphenylamino)-propanenitrile				3.1	8.7	3.4	1.1	1.1
2,6-Dichloro-4-nitroaniline						1.5	3.4	5.1
<b>Disperse orange 3 (4-(4-Nitrophenylazo)aniline), Dye # 6</b>								
Aniline					2.8	1.9	0.9	1.1
Nitrobenzene					2.8	1.9	0.9	
Nitroaniline						23.2	18.1	16.6
Diaminobenzene					2.3	2.6	4.1	
<b>Disperse yellow 37(3-[4-(2,6-Dichloro-4-nitrophenylazo)-N-ethylaniline]propionitrile), Dye# 7</b>								
Hydroxy toluene					0.7	7.6	1.5	0.6
Acetanilide						0.8	0.8	1.0
Methylhydroxy aniline						1.0	1.2	1.4
<b>DABITC (4-(4-Isothiocyantophenylazo)-N,N-dimethylaniline), Dye # 8</b>								
COS			3.4	11.6	1.8	2.0	0.3	
Thiourea			1.3		20.7	3.5	4.9	3.3
N,N-dimehylaniline					2.5	1.2	1.1	1.0
<b>Disperse Orange 25 (3-[N-Ethyl-4-(4-nitrophenylazo)phenylamino]propionitrile), Dye # 9</b>								
CH <sub>2</sub> = CHCN			57.6	4.6	1.9	0.9	0.3	
Aniline			0.9	0.4	0.3	0.1		
a-naphthol				4.4	4.0	4.3	4.1	3.1
Nitroaniline				0.9	0.4	0.3	0.1	
<b>Disperse Red 1 (N-Ethyl-N-(2-hydroxyethyl)-4-(4-nitrophenylazo)aniline), Dye # 10</b>								
Diaminobenzene			6.7	14.1	7.9	8.9	7.2	
N-ethyldiaminobenzene		12.9	14.7	9.3				
Aniline		1.8	7.3	10.6	2.3	1.4		

electron donating group weakened the phenyl nitrogen bond away from the donor group (bond B). Dyes # 5, 6, 8, 9, and 10 all share the presence of donor group on one side and acceptor group on the

other side and based on their TGA and DTG behavior, bond B is more easily broken to give nitrobenzene derivatives. For dye #7 it is the only dye that carries both donor groups on both sides, and as shown

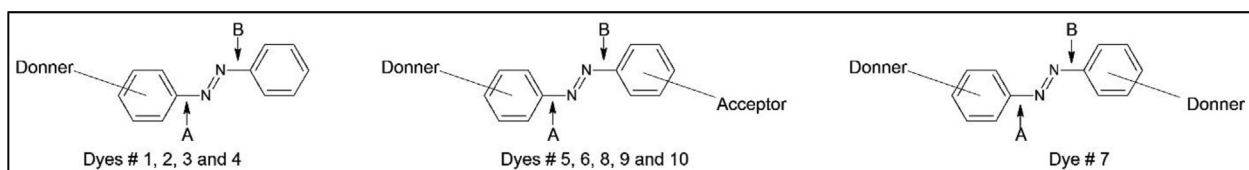


Fig. 6. Chemical bond assignment (A & B) with respect to donor and acceptor groups for the azobenzene dyes.

Table 3

Thermodynamics properties of the tested azo dyes as compared to the unsubstituted azobenzene.

Dye #	Bond order			Bond Dissociation Energy (KJ/mol)		D.M. (Debye)	$(\Delta H^\circ)$ N <sub>2</sub> Loss (KJ/mol)
	A	B	NN	A	B		
1	1.295	1.184	1.924	359.07	331.38	0.46	371.9
2	1.322	1.193	1.988	346.48	323.03	3.21	359.3
3	1.228	1.195	1.998	326.22	312.63	3.55	339.0
4	1.224	1.196	2.002	324.11	312.91	2.74	336.9
5	1.243	1.178	1.996	340.97	313.88	7.11	328.6
6	1.241	1.198	1.986	346.89	316.46	8.73	340.5
7	1.264	1.193	1.943	360.94	352.70	4.86	375.2
8	1.241	1.204	1.985	332.67	318.46	8.66	344.8
9	1.238	1.198	1.992	346.11	325.00	7.86	339.7
10	1.246	1.201	1.983	364.99	331.30	7.88	358.6
Azobenzene	1.194	1.194	2.026	313.15	313.156	0.02	325.9

in Figs. 2 and 6 and Table 1, this dye is the slowest in breaking down because the donor group equally strengthens both A and B bonds.

### 3.3. Computational assessment

All quantum chemical calculations and thermodynamic properties of the tested dyes were performed using the density functional theory (DFT) B97M-V with the 6-311 + G(2df,2p) [6-311G\*] basis set in the Spartan 18 program package (Wavefunction, Inc. Irvine, CA, U.S.A.). Bond order and bond dissociation energy of the azo group moiety as well as dipole moments and the enthalpy ( $\Delta H^\circ$ ) for the thermal loss of nitrogen molecules of all the tested dyes are shown in Table 3. In all the tested dyes, bond order and dissociation energy of B bonds (as shown in Fig. 6) were lower than that for the A bond, indicating that bond B is thermodynamically easier to breakdown than bond A. As it was mentioned before only dye #7 has donor groups on each side of the azobenzene structures and it was constant that it is the only dye with a relatively higher ( $\Delta H^\circ$ ) value than all the other dyes for losing an N<sub>2</sub> molecule (Table 3). Computational data are consistent with the experimental results for the TGA experiments and product identification using GCMS.

According to the experiments and computational studies, it appeared that the thermal degradation of the azo dyes took place in

two steps with the first step consisting of breaking the B bond and forming two free radicals, one as a phenyl radical and the other is an azo radical. The second step is the breaking the A bond and releasing a nitrogen molecule and the second phenyl radical as shown in Fig. 7.

Heat of reaction for the loss of N<sub>2</sub> gas listed in Table 3 is calculated based on the sum of the two steps shown in Fig. 7. Dyes #1–4 having only one donor group and no acceptor group, showed that bond B is weaker than bond A with dissociation energies ranging from 313 to 331 kJ/mol as compared to 324–359 kJ/mol for bond A. Intermolecular hydrogen bonding through tautomerism increased the dissociation energy of bond B. It can also be seen that electron donating groups increase the dissociation energy of bond B compared to the non-substituted azobenzene. The second group of dyes having a donor group on one side and an electron withdrawing group on the other side (Dyes #5, 6, 8, 9, and 10) also showed that bond B is weaker than bond A ranging from 313 to 331 kJ/mol compared to 333–365 kJ/mol for bond B and 313 kJ/mol for non-substituted azobenzene; none of these dyes have an intramolecular hydrogen bond. Dye #7 has a donor group on each side which resulted in increasing bond energy for both A and B bonds.

Products listed in Table 2 can be explained by the fact that initially formed organic free radicals which were formed in the initiation steps quickly proceeded to form other radicals during the propagation steps

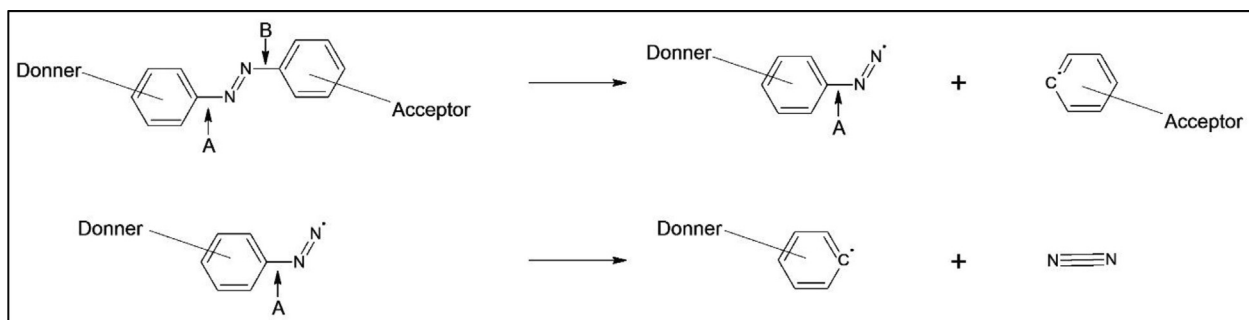


Fig. 7. Degradation of azo dyes to release nitrogen gas.

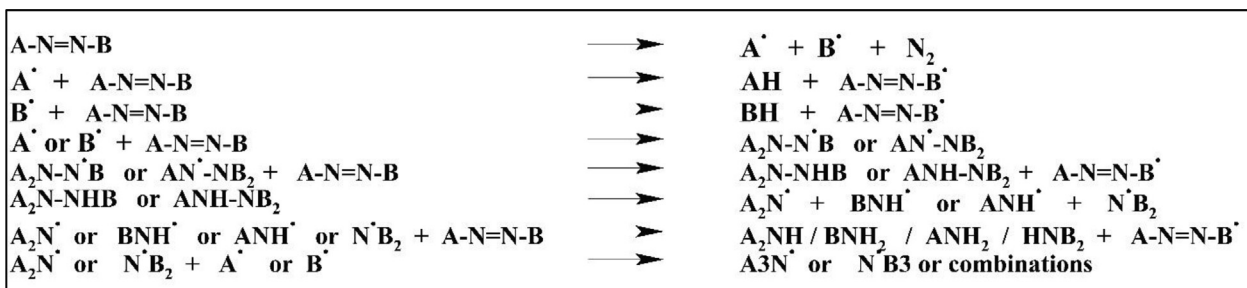


Fig. 8. Possible scheme for the thermal free radicals degradation of the azobenzene dyes for initiation, propagation, and termination steps.

by abstracting a hydrogen atom or an organic group to form new radicals and neutral molecules and finally all of the formed radicals were converted to neutral molecules at the termination step. GCMS analysis can only detect thermal products as neutral molecules, however, their radical precursors can easily be anticipated based on the chemical identification of the product. For example, the detection of benzene molecule predicted that phenyl radical was formed and then was converted to benzene by abstracting a hydrogen atom from the starting materials, forming a new radical and so on. Similarly, detection of phenol, nitrobenzene, or aniline can be interpreted as a product from phenol or nitrobenzene or aniline radicals that were produced in the initiation or propagation steps followed by abstracting hydrogen atoms from the parent compound. A summary of all the possible initiation, propagation, and termination steps are shown in Fig. 8.

#### 4. Conclusion

Data obtained experimentally by TGA/GCMS and theoretically by quantum mechanics confirmed each other and support the proposed thermal degradation mechanisms of the examined azobenzene dyes by designating the weak bonds and their associated bond breaking products. Thermal stability of these azobenzene dyes as a function of starting decomposition temperature and remaining of azo group depending upon the temperature and the presence of donor or accepting groups. Thermal weight losses occurred in the same order of DTG values. These values refer to the order of stability of the remainder parts keeping azo groups at elevated temperatures and decomposed in the second step. These finding provided important knowledge about the process of thermal degradation of these dyes and consequently the temperature range of its thermal stability before decomposition and releasing of suspected carcinogenic aromatic amines. Free-radical pathways are the dominate mechanisms for thermal degradation of azo dyes. The general reaction conditions consisting of high temperature, gas phase and an absence of acidic or basic catalysts are favorable for free-radical behavior. Thermal degradation of the tested azobenzene dyes demonstrated that the stability depends on the substituted groups and their position in the dye structures.

#### Declaration of Competing Interest

The authors declare that they have no known competing financial interests or personal relationships that could have appeared to influence the work reported in this paper.

#### Acknowledgments

This publication was made possible in part, by research infrastructure support from grant number 2G12MD007605 from the National Institutes of Health NIMHD/NIH.

#### References

- [1] A. Bafana, S.S. Devi, T. Chakrabarti, Azo dyes: past, present and the future, *Environ. Rev.* 19 (2011) 350–370.
- [2] Azo Dyes Market 2019 Industry Size by Global Major Companies Profile, press release, Aug 7, 2019.
- [3] M. Šuleková, M. Smrčková, A. Hudák, M. Heželová, M. Fedorová, Organic coloring agents in the pharmaceutical industry, *Folia* 6 (2017) 32–46.
- [4] K.T. Chung, Azo dyes and human health: a review, *J. Environ. Sci. Health C* 34 (2016) 233–261.
- [5] L.I. Khayyat, A.E. Essawy, J.M. Sorour, A. Soffar, Sunset yellow and Allura red modulate BCL2 and COX2 expression levels and confer oxidative stress-mediated renal and hepatic toxicity in male rats, *Peer J.* 6 (2018) e5689.
- [6] H. Tian, J. Zhang, *Photochromic Materials: Preparation, Properties and Applications*, Wiley-VCH, Weinheim, 2016.
- [7] T. Yamaguchi, Y. Kobayashi, J. Abe, Fast negative photochromism of 1, 1'-binaphthyl-bridged phenoxyl-imidazolyl radical complex, *J. Am. Chem. Soc.* 138 (2016) 906–913.
- [8] I. Ayadi, Y. Souissi, I. Jlassi, F. Peixoto, W. Mnif, Chemical synonyms, molecular structure, and toxicological risk assessment of synthetic textile dyes: a critical review, *J. Develop. Drugs* 5 (2016) 151.
- [9] L.H. Ahlstrom, C.S. Eskilsson, E. Björklund, Determination of banned azo dyes in consumer goods, *Trends Anal. Chem.* 24 (2005) 49–56.
- [10] I.I. Arslan, A. Bacioglu, T. Tuhkanen, D. Bahnemann, H<sub>2</sub>O<sub>2</sub>/UV-C and Fe<sup>2+</sup>/H<sub>2</sub>O<sub>2</sub>/UV-C versus TiO<sub>2</sub>/UV-A treatment for reactive dye wastewater, *J. Environ. Eng.* 126 (2000) 903–911.
- [11] P. Moller, H. Wallin, Genotoxic hazards of azo pigments and other colorants related to 1-phenylazo-2-hydroxynaphthalene, *Mutat. Res.* 462 (2000) 13–30.
- [12] K. Golka, S. Koppes, Z.W. Myslak, Carcinogenicity of azo colorants: influence of solubility and bioavailability, *Toxicol. Lett.* 151 (2004) 203–210.
- [13] K.T. Chung, Mutagenicity and carcinogenicity of aromatic amines metabolically produced from azo dyes, *Environ. Carcin. Ecotox. Rev.* C18 (2000) 51–74.
- [14] F. Rafii, J.D. Hall, C.E. Cerniglia, Mutagenicity of azo dyes used in foods, drugs, and cosmetics before and after reduction by Clostridium species from the human intestinal tract, *Food. Chem. Toxicol.* 35 (1997) 897–901.
- [15] T. Nguyen, M.A. Saleh, Detection of azo dyes and aromatic amines in women undergarment, *J. Environ. Sci. Health, Part A* 51 (2016) 744–753.
- [16] C. Lavanyal, R. Hankar, S. Chhikara, S. Sheoran, Degradation of toxic dyes: a review, *Int. J. Curr. Microbiol. App. Sci.* 3 (2014) 189–199.
- [17] V.M. Correia, T. Stephenson, S.J. Judd, Characterizations of textile wastewaters-a review, *Environ. Technol.* 15 (1994) 917–929.
- [18] I. Mustafa, D.T. Sponza, Fate and toxicity of azo dye metabolites under batch long-term anaerobic incubations, *Enzyme Microb. Technol.* 40 (2007) 934–939.
- [19] M.C. Tomei, D.M. Angelucci, A.J. Daugulis, Sequential anaerobic-aerobic decolorizations of a real textile wastewater in a two-phase partitioning bioreactor, *Sci. Total Environ.* 573 (2016) 585–593.
- [20] P.J. Cai, X. Xiao, Y.R. He, W.W. Li, J. Chu, C. Wu, Anaerobic bio decolorization mechanism of methyl orange by *Shewanella oneidensis* MR-1, *Appl. Microbiol. Biotechnol.* 93 (2012) 1769–1776.
- [21] W. Zhang, M. Chen, S. Zhang, Y. Wang, Designation of a solar falling-film photochemical hybrid system for the decolorization of azo dyes, *Energy* 197 (2020) 117–182.
- [22] W.M. Alabdraba, A. Albayati, Biodegradation of azo dyes, a review, *Int. J. Environ. Eng. Nat. Resour.* 1 (2014) 179–189.
- [23] P.S. Patil, S. Phugare, S. Jadhav, J.P. Jadhav, Communal action of microbial cultures for Red HE3B degradation, *J. Hazard. Mater.* 181 (2010) 263–270.
- [24] B. Marcandalli, Photochemical trans-cis Isomerization of some 4diethylaminoazobennenes, *Dyes Pigm.* 14 (1990) 79–88.
- [25] E.P. Chagas, L.R. Durrant, Decolorization of azo dyes by *Phanerochaete chrysosporium* and *Pleurotus sajorajaju*, *Enzyme Microb. Technol.* 29 (2001) 474–477.
- [26] R. Bras, M. Ferra, M. Isabel, H.M. Pinheiro, I.C. Goncalves, Batch tests for assessing decolorization of azo dyes by methanogenic and mixed cultures, *J. Biotech.* 89 (2001) 155–162.
- [27] M. Adosinda, M. Martins, N. Lima, S. Ailvestre, M. Queiroz, Comparative studies of fungal degradation of single or mixed bio accessible reactive azo dyes, *Chemosphere* 52 (2003) 967–973.